

## Article

# Darcy–Brinkman Double Diffusive Convection in an Anisotropic Porous Layer with Gravity Fluctuation and Throughflow

Gangadharaiah Yeliyur Honnappa <sup>1</sup>, Manjunatha Narayanappa <sup>2</sup>, Ramalingam Udhayakumar <sup>3,\*</sup>,  
Barakah Almarri <sup>4,\*</sup>, Ahmed M. Elshenhab <sup>5,6</sup> and Nagarathnamma Honnappa <sup>7</sup>

<sup>1</sup> Department of Mathematics, RV Institute of Technology & Management, Bengaluru 560076, India

<sup>2</sup> Department of Mathematics, School of Applied Sciences, REVA University, Bengaluru 560064, India

<sup>3</sup> Department of Mathematics, School of Advanced Sciences, Vellore Institute of Technology, Vellore 632014, India

<sup>4</sup> Department of Mathematical Sciences, College of Sciences, Princess Nourahbint Abdulrahman University, P.O. Box 84428, Riyadh 11671, Saudi Arabia

<sup>5</sup> School of Mathematics, Harbin Institute of Technology, Harbin 150001, China

<sup>6</sup> Department of Mathematics, Faculty of Science, Mansoura University, Mansoura 35516, Egypt

<sup>7</sup> Department of Mathematics, Dr. Ambedkar Institute of Technology, Bengaluru 560056, India

\* Correspondence: udhayakumar.r@vit.ac.in (R.U.); bjalmarri@pnu.edu.sa (B.A.)

**Abstract:** The influence of the throughflow and gravity fluctuation on thermosolutal convection in an anisotropic porous bed with the Darcy–Brinkman effect is considered numerically. The critical Rayleigh numbers for the onset of stationary and oscillatory modes have been found via linear instability analysis. The impact of various gravitational functions in the presence of throughflow on stability is studied. The analysis has been carried out for decreasing and increasing gravity fluctuations. The convective problem has been numerically analyzed using a single-term Galerkin approach. The results show that the mechanical anisotropy parameter and Lewis number have a destabilizing effect, while the thermal anisotropy parameter, Darcy number, solutal Rayleigh number, throughflow parameter, and gravity parameter have a stabilizing effect on stationary and oscillatory convection. It is clear that the system changes in a way that makes it more stable for case (iii) gravity fluctuation and more unstable for case (iv) gravity fluctuation.

**Keywords:** double-diffusive convection; Brinkman model; anisotropy; throughflow; changeable gravity

**MSC:** 76Rxx; 74E10; 37L65



**Citation:** Yeliyur Honnappa, G.; Narayanappa, M.; Udhayakumar, R.; Almarri, B.; Elshenhab, A.M.; Honnappa, N. Darcy–Brinkman Double Diffusive Convection in an Anisotropic Porous Layer with Gravity Fluctuation and Throughflow. *Mathematics* **2023**, *11*, 1287. <https://doi.org/10.3390/math11061287>

Academic Editors: Katta Ramesh and Rama Subba Reddy Gorla

Received: 2 February 2023

Revised: 3 March 2023

Accepted: 3 March 2023

Published: 7 March 2023



**Copyright:** © 2023 by the authors. Licensee MDPI, Basel, Switzerland. This article is an open access article distributed under the terms and conditions of the Creative Commons Attribution (CC BY) license (<https://creativecommons.org/licenses/by/4.0/>).

## 1. Introduction

Many fields, including the petroleum industry, binary mixture solidification, and solute movement in water-saturated soils, significantly benefit from the investigation of double-diffusive convection in porous media. The Earth's oceans, crystallization processes, electrochemistry, moisture movement via fibrous insulation, geophysical phenomena, and magma chambers are further examples. Researchers have been interested in convective heat transfer in porous media for many years. This interest was sparked by a variety of thermal engineering applications in several fields, including the modeling of packed spherical beds, thermal insulation engineering, geophysics, groundwater hydrology, coal combustors, petroleum reservoirs, and others. Due to its applications in engineering, geophysics, and bottom hydrodynamics, the throughflow effect on double-diffusive convection in a porous media is a crucial concept. The mushy zone, which is thought of as a porous layer with a double-diffusive origin, appears in concentrated alloys and is thought to play a significant role in the directed solidification of those alloys. Layer height causes the fundamental state

temperature profile of throughflow to shift from linear to nonlinear, which has a substantial impact on the system's stability.

Anisotropy in porous configuration, caused by a quasi-arrangement of porous beds or fibers, is abundant in nature and has numerous practical uses. Anisotropic porous media include rock, soil, and fiber-insulating materials. Castinel and Combarous [1] were the first to investigate thermal instability in a porous matrix layer with anisotropic permeability. They determined the conditions for the onset of convection both empirically and conceptually. Epherre [2] expanded the stability investigation on anisotropic porous beds to thermal diffusivity effects. Kvernold and Tyvand [3] investigated nonlinear instability caused by a thermal expansion in a porous bed, and they theoretically found the condition for convective stability. Later, Malashetty and Swamy [4], Govinder [5], Shivakumara et al. [6], Degan et al. [7], Payne et al. [8], Rees and Postelnicu [9], and Yadav and Kim [10] investigated the issue. Mahajan and Nandal [11] extended this problem to thermosolutal convection with Coriolis and Brinkman effects.

The gravitational field has been shown to fluctuate in elevation from its planes in a wide range of relevant situations. We generally overlook this gravity difference in laboratory studies and assume that gravity force is steady. To a considerable degree, however, it is necessary to understand the changing quality of gravity. In this regard, the examination of instability in a porous bed with fluctuating gravitational forces seems critical. However, research into the effects of a changing gravity field in a porous media is quite restricted. Alex and Patil [12] have investigated the effect of the linear type of gravity fluctuation on the initiation of flow in a porous bed and discovered that decreasing the fluctuation improved the arrangement's stability. Rionero and Straughan [13] looked into the impact of different types of gravity fluctuation at the start of penetrative convective flow in a porous bed. A single-layer system with gravity variation and throughflow in a Brinkman-type porous media was investigated by Gangadharaiah et al. [14]. Suma et al. [15] and Gangadharaiah et al. [16] used the perturbation method to analyze the joint impact of the Peclet number and gravity fluctuation on the commencement of instability in a porous bed by considering the linear variation in gravity with height. Yadav [17] expanded this problem for surjection and injection and showed that the upward throughflow parameter enables the postponement of the commencement of the flow. Recently, Gangadharaiah et al. [18] investigated the impact of gravity fluctuation on the stability of double-diffusive problems in a fluid layer with throughflow. The researcher may refer to Mahabaleshwar et al. [19], Mahajan and Tripathi [20], Yadav et al. [21], Yadav et al. [22], and Yadav [23] for additional information. Double-diffusive convection in a porous media exposed to temperature/gravity modulation was explored by Siddheshwar et al. [24]. In an anisotropic porous layer with an internal heat source that is heated and salted from below, Bhadauria [25] investigated double-diffusive convection. In the presence of a concentration-based internal heat source, Deepika et al. [26] investigated the start of double-diffusive convection in a horizontal fluid-saturated porous layer. Using the Landau model, Gaikwad and Preeti [27] investigated how throughflow and gravity modulation affected double-diffusive convection in porous media saturated with a couple-stress fluid.

According to a review of the literature, throughflow impacts on the solutal convective flow in a porous bed with Darcy–Brinkman effects and an unequal gravity variation have not yet been explored. Such studies might be very helpful in the understanding of massive movements, such as the processing of materials, pollutant passage in saturated soils, the Earth's crust, atmosphere, and ocean, as well as fuel penetration, and crystal formation, for which both injection and suction can be crucial to controlling convective instability. The present work's major goal is to analyze how throughflow and a changing gravity field interact to affect the onset of Darcy–Brinkman's solutal convective motion in a porous bed to understand the significance of such an issue. The plan of this research paper is as follows: In Section 2, we describe the considered problem. In Section 3, the analysis of linear instabilities is performed. The technique of the solution is described in Section 4.

The numerical results and discussions are presented in Section 5. The research ends with conclusions in Section 6.

### 2. Materials and Methods

The simplified physical model of double-diffusive convection, shown in Figure 1, is an infinite anisotropic bed enclosed by surfaces  $z = 0$  and  $z = d$ . A cartesian frame of reference is chosen in such a way that the origin lies on the lower plane and the  $z$ -axis is vertically upward. Let  $\Delta T$  &  $\Delta C$  represent differences of the temperature and concentration, respectively, where  $T_0, C_0$  are the temperature and concentration of the upper plates, respectively. The physical configuration of the model is reported in Figure 1, with a vertical throughflow velocity  $w_0$  and gravity effect  $g(z) = (1 + \delta h(z))g$ . The Darcy–Brinkman model for the motion of the binary fluid mixture, according to the Boussinesq approximation, are

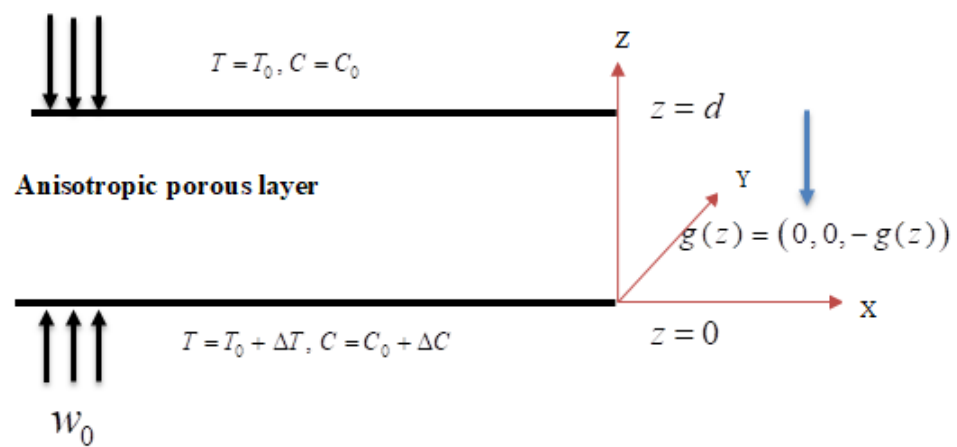


Figure 1. Physical model.

The flow governing equations are

$$\nabla \cdot \vec{V} = 0 \tag{1}$$

$$\rho_0 \left( \frac{\partial \vec{V}}{\partial t} + (\vec{V} \cdot \nabla) \vec{V} \right) = -\nabla p - \frac{\mu}{K} \vec{V} + \mu \nabla^2 \vec{V} - \rho g(z) \hat{k} \tag{2}$$

$$\frac{\partial T}{\partial t} + (\vec{V} \cdot \nabla) T = \kappa \nabla^2 T \tag{3}$$

$$\frac{\partial C}{\partial t} + (\vec{V} \cdot \nabla) C = \kappa_S \nabla^2 C \tag{4}$$

$$\rho = \rho_0 \{ 1 + \alpha_C (C - C_0) - \alpha_T (T - T_0) \} \tag{5}$$

The boundary conditions are

$$C = C_0 + \Delta C, \quad T = T_0 + \Delta T \quad \text{at } z = 0 \tag{6}$$

$$C = C_0, \quad T = T_0 \quad \text{at } z = d \tag{7}$$

The basic state of the fluid is

$$(u, v, w, T, p, \rho, C) = [0, 0, w_0, T_b(z), p_b(z), \rho_b(z), C_b(z)] \tag{8}$$

Infinite disturbances of the form are added to test the stability of the basic solution

$$(u, v, w, T, p, \rho, C) = [0, 0, w_0, T_b(z), p_b(z), \rho_b(z), C_b(z)] + [u', v', w', T', p', \rho', C'] \quad (9)$$

where the disturbed quantities are those over their equilibrium counterparts that are primed. Substituting Equation (9) into Equations (1)–(5) and operating the curl twice on Equation (2), eliminate the pressure term from it to obtain dimensionless equations as

$$\frac{1}{Pr} \frac{\partial}{\partial t} \nabla^2 w + \left( \nabla_1^2 + \frac{1}{\xi} \frac{\partial^2}{\partial z^2} \right) w - Da \nabla^4 w = \left\{ R \nabla_1^2 T + Rs \nabla_1^2 C \right\} G(z) \quad (10)$$

$$\frac{\partial T}{\partial t} = \nabla_1^2 T + w f_T(z) \quad (11)$$

$$\frac{\partial C}{\partial t} = Le \nabla_1^2 C + w f_C(z) \quad (12)$$

where

$$a^2 = l^2 + m^2, \nabla_1^2 = \frac{\partial^2}{\partial x^2} + \frac{\partial^2}{\partial y^2} \text{ and } \nabla^2 = \nabla_1^2 + \frac{\partial^2}{\partial z^2}$$

$$R = \frac{\alpha g \Delta T d^3}{\nu \kappa} \text{ is the thermal Rayleigh number}$$

$$Rs = \frac{\rho_s g \Delta C d^3}{\nu \kappa_s} \text{ is the solutal Rayleigh number}$$

$$Le = \frac{\kappa_s}{\kappa} \text{ is the Lewis number}$$

$$Pr = \frac{\nu}{\kappa} \text{ is the Prandtl number}$$

$$G(z) = 1 + \delta h(z) \text{ is the gravity function}$$

$$h(z) \text{ is the gravity fluctuation}$$

$$f_T(z) = \frac{-Qe^{Qz}}{e^Q - 1} \text{ is the dimensionless function}$$

$$f_C(z) = -Le Q \left( \frac{e^{Le Qz}}{1 - e^{Le Q}} \right) \text{ is the dimensionless function}$$

$$Q \text{ is the throughflow parameter}$$

### 3. Linear Stability Analysis

To study linear stability analysis according to the solution of the eigenvalue problem defined by Equations (10)–(12) and subject to the boundary condition, use time-dependent periodic disturbances in the horizontal plane:

$$(w, T, C) = \{W(z), \Theta(z), \Phi(z)\} \exp[i(lx + my) + \sigma t] \quad (13)$$

On applying of Equation (13) into Equations (10)–(12), we can write:

$$\left\{ Da \left( D^2 - a^2 \right) - \frac{\sigma}{Pr} \right\} \left( D^2 - a^2 \right) W - \left( \frac{1}{\xi} D^2 - a^2 \right) W = \left\{ R a^2 \theta - Rs a^2 S \right\} G(z) \quad (14)$$

$$\left( D^2 - \eta a^2 - QD - \sigma \right) \theta = W f_T(z) \quad (15)$$

$$\left( D^2 - a^2 - \sigma Le \right) S = W f_C(z) \quad (16)$$

The linearized boundary conditions are:

$$W = DW = \theta = S = 0 \text{ at } z = 0 \text{ and } z = 1 \quad (17)$$

where  $D = \frac{d}{dz}$ .

#### 4. Technique of Solution

Using the Gelarkin method, the eigenvalue problem described by Equations (14)–(16) is solved. To achieve a non-trivial solution to the eigenvalue problem with assumed boundary conditions, assume the solution of the form

$$W = A_1 \sin(n\pi z), \Theta = A_2 \sin(n\pi z), \Phi = A_3 \sin(n\pi z) \tag{18}$$

Substituting (18) into (14)–(16) and integrating between  $z = 0$  and  $z = 1$ , the following matrix equations are obtained:

$$\begin{bmatrix} -(n^2\pi^2 + a^2) & R P_1 & R s P_1 \\ P_2 & -(n^2\pi^2 + a^2 + \sigma) & -(n^2\pi^2 + a^2) \\ R s P_3 L e & -L e (n^2\pi^2 + a^2) & -(n^2\pi^2 + a^2 + \delta L e \sigma) \end{bmatrix} \begin{bmatrix} A_1 \\ A_2 \\ A_3 \end{bmatrix} = \begin{bmatrix} 0 \\ 0 \\ 0 \end{bmatrix} \tag{19}$$

$$R^c = \frac{-\Delta \{ (D a \Delta + \sigma) (\Delta + D a \delta L e \sigma) - L e \Delta^2 \}}{P_1 P_2 \{ (-D a \Delta - \delta L e \sigma) + L e \Delta \}} + \frac{R s P_3 \{ -\Delta D a + L e \Delta + \sigma \}}{P_2 \{ (-\Delta D a - \delta L e \sigma) + L e \Delta \}} \tag{20}$$

where  $\Delta = n^2\pi^2 + a^2$ ,  $P_1 = \int_0^1 a^2 G(z) \sin(n\pi z) dz$ ,  $P_2 = \frac{1}{L e} a^2 R s \int_0^1 f_T(z) \sin(n\pi z) G(z) dz$ , and  $P_3 = \int_0^1 f_C(z) \sin(n\pi z) dz$ .

##### 4.1. Stationary State

The values of the thermal Rayleigh number and the corresponding wave number of the system for a stationary mode are obtained by using the growth rate parameter  $\sigma = 0$

$$(R^c)^{st} = \frac{1}{a^2} \left[ \left\{ \frac{n^2\pi^2}{\xi} + a^2 + D a (n^2\pi^2 + a^2)^2 \right\} (n^2\pi^2 + \eta a^2) \right] + L e R s \frac{(n^2\pi^2 + \eta a^2)}{(L e + n^2\pi^2 + a^2)} \tag{21}$$

##### 4.2. Limiting Case

For  $D a = 0$  and  $G(z) = 1$ , Equation (21) reduces to

$$(R^c)^{st} = \frac{1}{a^2} \left[ \left\{ \frac{n^2\pi^2}{\xi} + a^2 \right\} (n^2\pi^2 + \eta a^2) \right] + L e R s \frac{(n^2\pi^2 + \eta a^2)}{(L e + n^2\pi^2 + a^2)}$$

which is the result obtained by Malashetty and Biradar [28].

##### 4.3. Oscillatory State

For the corresponding wave number of the system for the oscillatory mode of convection, we now set  $\sigma = i \sigma_i$  in Equation (20) and the oscillatory mode reduces it to

$$(R^c)^{os} = \frac{\left\{ \frac{n^2\pi^2}{\xi} + a^2 \right\} (n^2\pi^2 + \eta a^2) \{ \Delta^2 (1 - L e D a) \} + R s \{ \Delta^2 D a (1 - L e) - L e \delta \sigma_i^2 \}}{\left\{ \Delta^2 (1 - L e)^2 + L e^2 \delta^2 \sigma_i^2 \right\}} \tag{22}$$

where the oscillatory frequency is  $\sigma_i^2 = \frac{a^2 R s (n^2\pi^2 + L e a^2)}{(L e + \delta n^2\pi^2 + a^2)} + \frac{\delta \Delta^2 D a (1 - L e)}{1 + L e^2 \delta^2}$ .

The critical Rayleigh number,  $R^c$ , values are generated from  $(R^c)^{st}$  and  $(R^c)^{os}$  for corresponding values of wavenumber  $a$ .

#### 5. Results and Discussion

In this section, we discuss the effects, numerically and graphically, of the parameters in the governing equations on the onset of double-diffusive convection described by Darcy and Brinkman in an anisotropic porous bed. The stationary and oscillatory expressions for different values of the parameters, such as the gravity parameter, the mechanical anisotropic parameter, the Lewis number, the Darcy number, the thermal anisotropic parameter, the

throughflow parameter, and the solute Rayleigh number, with different gravity fluctuations, are computed, and the results are depicted in the figures. The study focused on two specific types of gravity fluctuations: 1. Decreasing gravity fluctuations: case (i)  $h(z) = -z$ , case (ii)  $h(z) = -z^2$ , and case (iii)  $h(z) = -(e^z - 1)$ . 2. Increasing gravity fluctuations: case (iv)  $h(z) = e^z$  case(v)  $h(z) = z$ , and case (vi)  $h(z) = \log(1 + z)$ . The critical values  $R^c$  and  $a^2$  with  $\delta$ , when throughflow is ( $Q = 0$ ) and solute concentration is ( $Rs = 0$ ), are computed, and discovered to accord well with Rionero and Straughan [13] (see Table 1).

**Table 1.** Effect of  $R^c$  and  $a^2$  with  $\delta$  with  $Q = Da = Rs = 0$  for two types of gravity scenarios.

$h(z)$	$\delta$	Present Work		Rionero and Straughan [13]	
		$R^c$	$a^2$	$R^c$	$a^2$
$-z$	0	39.477	9.871	39.478	9.870
	1	77.050	10.208	77.080	10.209
	1.5	132.020	12.313	132.020	12.314
	1.8	189.904	17.197	189.908	17.198
	1.9	212.286	19.475	212.281	19.470
$-z^2$	0	39.478	9.872	39.478	9.870
	0.2	41.832	9.873	41.832	9.874
	0.4	44.455	9.885	44.455	9.887
	0.6	47.389	9.916	47.389	9.915
	0.81	50.682	9.962	50.682	9.961
			54.390	10.035	54.390

Figures 2 and 3 show, for various values of the throughflow parameter  $Q$ , the fundamental temperature gradient  $f_T(z)$  and fundamental concentration gradient  $f_C(z)$  against the depth of the porous bed. It is noticed that the highest values of the temperature and concentration gradients occur at the lower boundary ( $z = 0$ ) for each quantity of downward throughflow. The temperature and concentration gradients at the bottom, however, are the lowest for each parameter, determining the amount of upward throughflow.

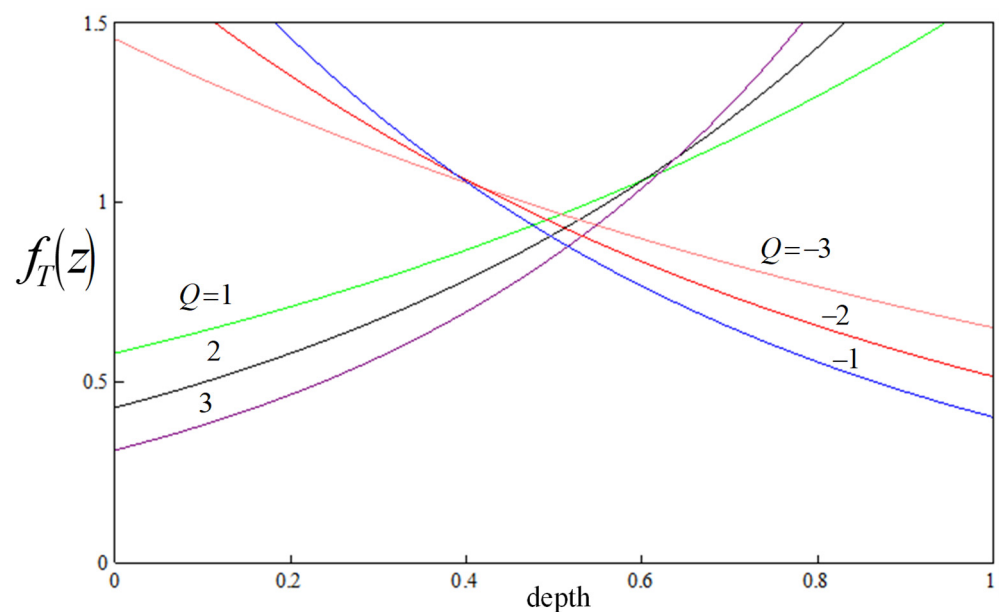


**Figure 2.** Plot of  $f_T(z)$  with depth for different values of  $Q$  with  $Le = 0.5, Rs = 10, Da = 0.1, \zeta = 0.5, \eta = 0.5,$  and  $\delta = 0.5$ .

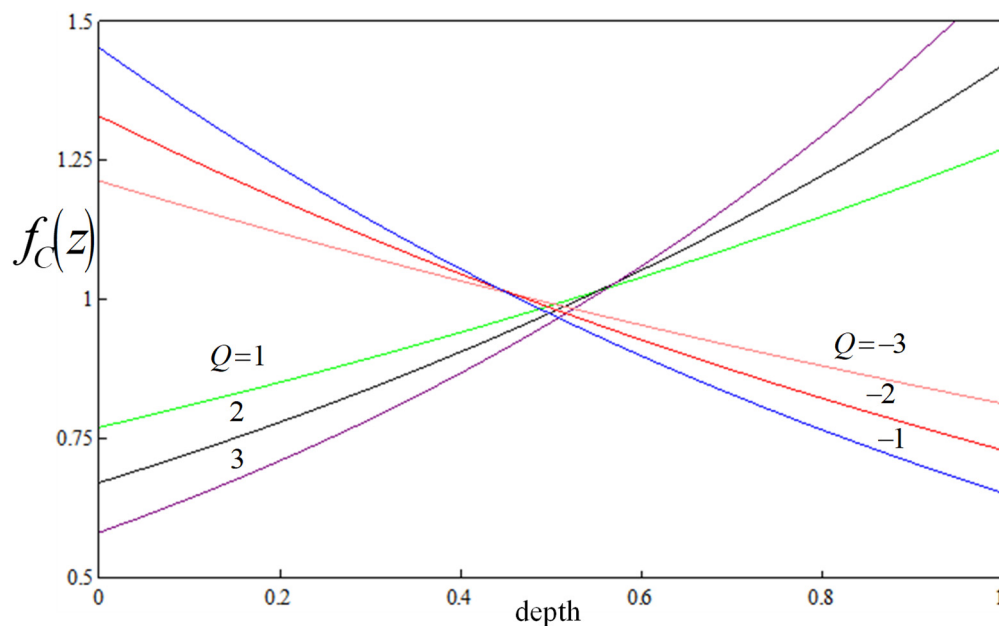


**Figure 3.** Plot of  $f_C(z)$  with depth, taking different values of throughflow parameters with  $Le = 0.5$ ,  $Rs = 10$ ,  $Da = 0.1$ ,  $\zeta = 0.5$ ,  $\eta = 0.5$  and  $\delta = 0.5$ .

Figure 4 illustrates the effect of  $R^c$  in both stationary and oscillatory modes with respect to the gravity parameter  $\delta$ . The results indicate that lower values of  $R^c$  are needed for convection motion, because as  $\delta$  values rise,  $R^c$  decreases. This occurs because a rise in the value of  $\delta$  raises the gravity in the case of a growing gravitational field; hence, convection starts more quickly. However, with decreasing types of gravitational field,  $R^c$  rises as the values of  $\delta$  increases. Furthermore, in case (iii), the gravitational field is more stable when compared to the remaining types of gravity fluctuation.

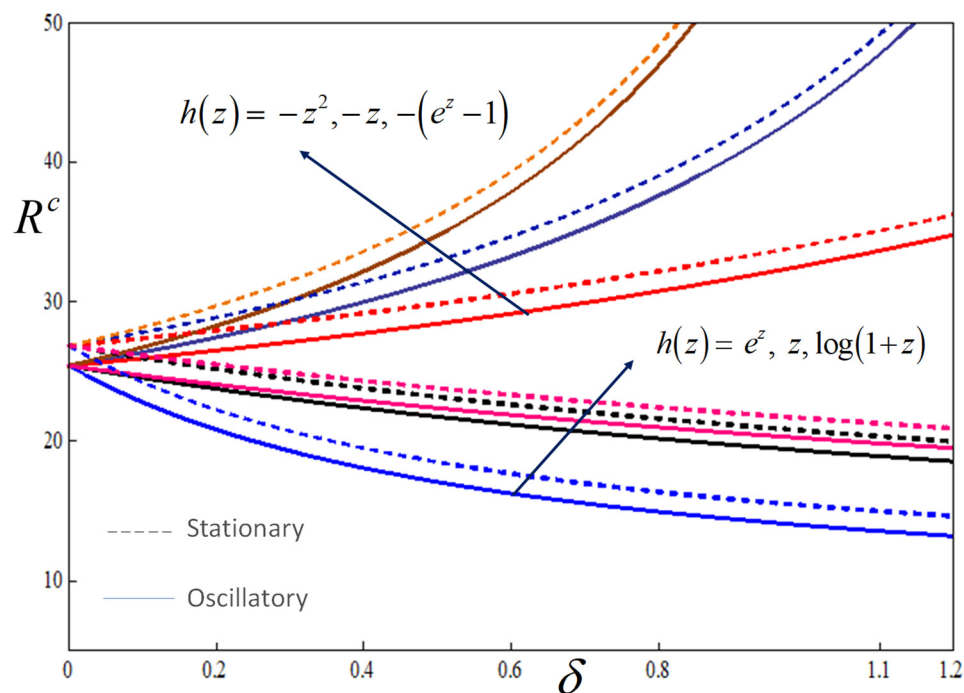


**Figure 4.** Plot of  $R^c$  versus  $\delta$  for different scenarios of gravity with  $Le = 0.5$ ,  $Rs = 10$ ,  $Da = 0.1$ ,  $\zeta = 0.5$ ,  $\eta = 0.5$  and  $\delta = 0.5$ .

Figures 5 and 6 display the deviance of  $R^c$  with  $Q$  for all categories of gravity function with  $Da = 100$  (Rayleigh Bénard convection) and  $Da = 0$  (Horton–Rogers–Lapwood convection), respectively. The results in Figure 5 indicate that in the presence of  $\delta$ , the throughflow term has a stabilizing impact and the plot of  $R^c$  is symmetric about  $Q = 0$ . In both cases of upward and downward throughflow, the flow with  $\delta = 0$  is more unstable than the flow with  $\delta = 0.5$  (see Figure 7). In the case of the Horton–Rogers–Lapwood convection with  $Da = 0$ , we note that  $|R^c|$  decreases with  $|Q|$  for all categories of gravity function. Hence, the configuration has destabilized with  $|Q|$ . Additionally, it was discovered that the effect of the throughflow parameter is more consistent for  $h(z) = -(e^z - 1)$  in contrast to other cases.

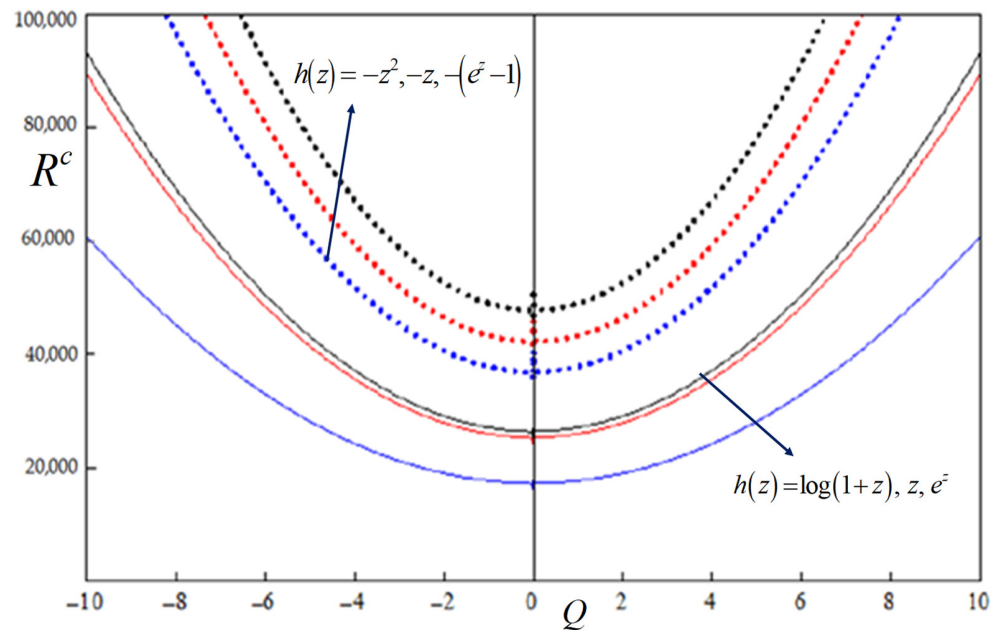


Figure 5. Plot of  $R^c$  versus  $Q$  for different scenarios of gravity with  $Le = 0.5$ ,  $Rs = 10$ ,  $Da = 100$ ,  $\xi = 0.5$ ,  $\eta = 0.5$  and  $\delta = 0.5$ .

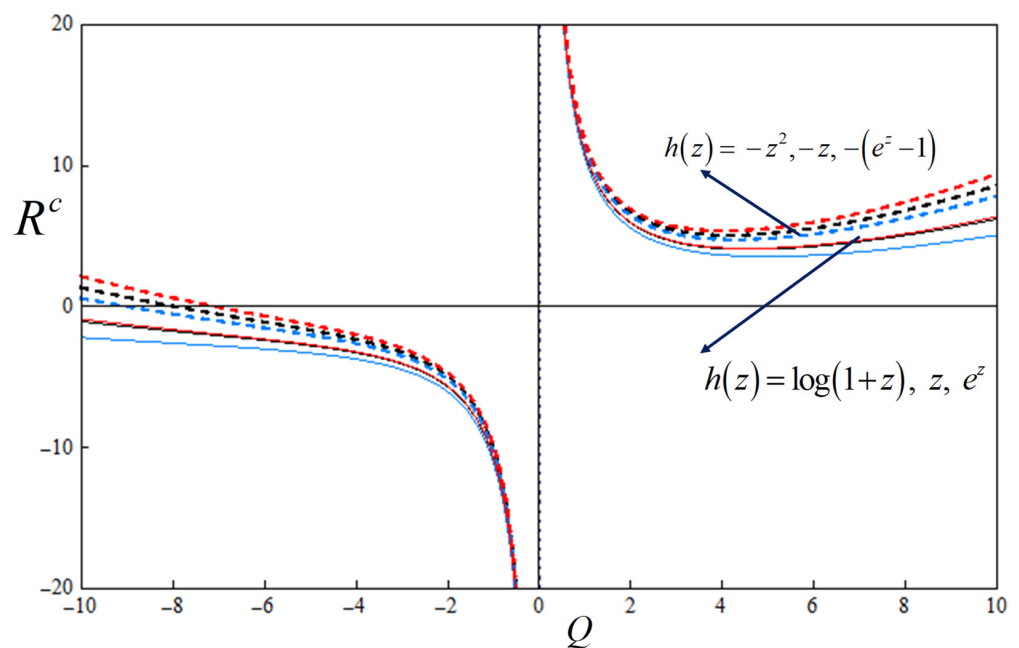
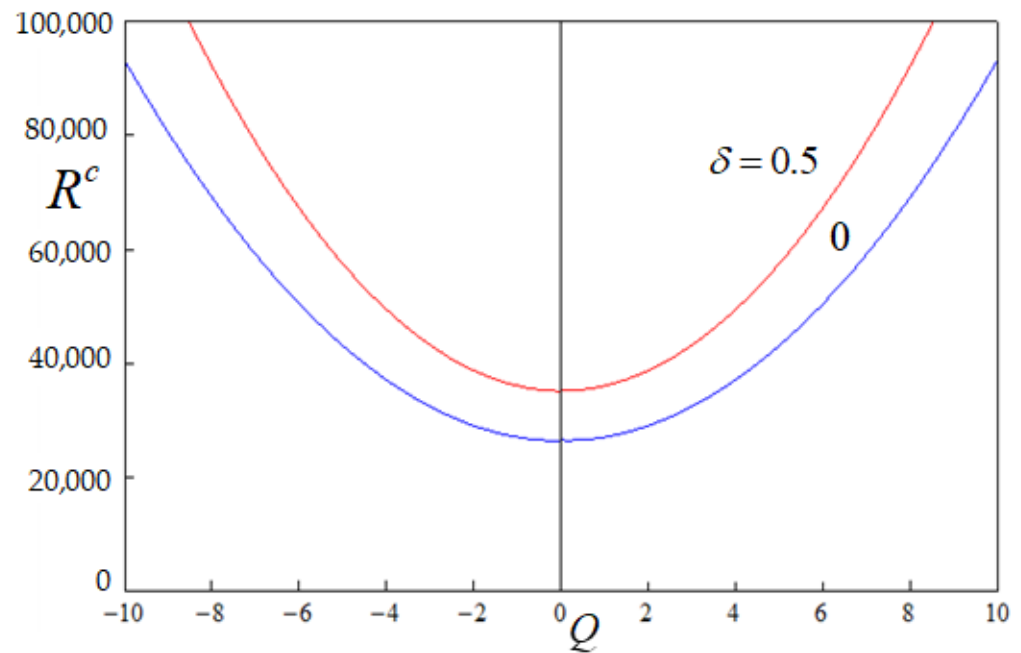
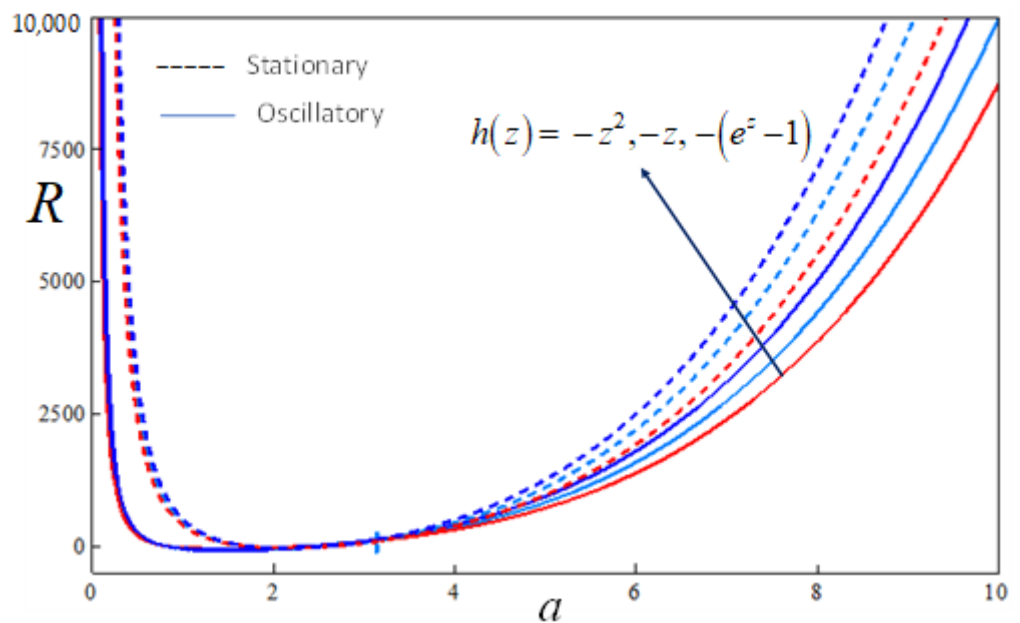


Figure 6. Plot of  $R^c$  versus  $Q$  for different scenarios of gravity with  $Le = 0.5$ ,  $Rs = 10$ ,  $Da = 0$ ,  $\xi = 0.5$ ,  $\eta = 0.5$  and  $\delta = 0.5$ .



**Figure 7.** Plot of  $R^c$  versus  $Q$  for two values of  $\delta$  for case (i) of gravity variation with  $Le = 0.5$ ,  $Rs = 10$ ,  $Da = 100$ ,  $\zeta = 0.5$  and  $\eta = 0.5$ .

Figures 8 and 9 represents the neutral stability curves for all six types of gravity function when  $Rs = 10$  and  $Le = 5$ . For stationary modes, the marginal stability curves will shift upwards; hence, stationary modes are more consistent than oscillatory modes. It should also be emphasized that the configuration is far more consistent for  $h(z) = -(e^z - 1)$  and the most inconsistent for  $h(z) = -z^2$ , the scenario of a decreasing type of gravity variation, whereas, in the case of increasing types of gravitational field variation, the configuration is far more consistent with the gravity scenario  $h(z) = \log(1 + z)$  and the most inconsistent for gravity scenario  $h(z) = e^z$ .



**Figure 8.** Plot of  $R$  versus  $a$  for different cases of gravity variation when  $Le = 0.5$ ,  $Rs = 10$ ,  $Da = 0.1$ ,  $\zeta = 0.5$ ,  $\eta = 0.5$  and  $\delta = 0.5$ .

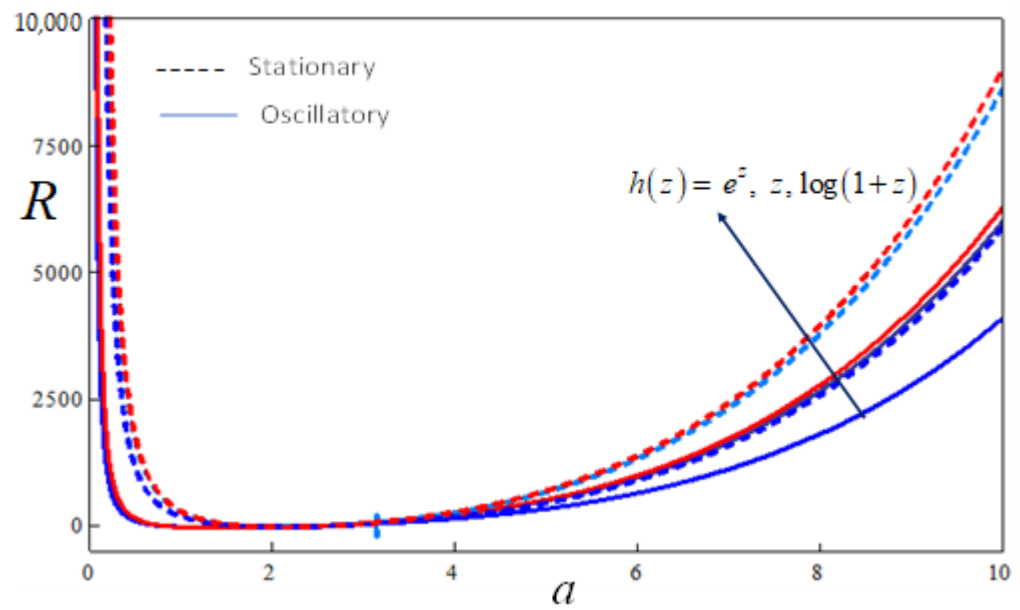


**Figure 9.** Plot of  $R$  versus  $a$  for different cases of gravity variation when  $Le = 0.5, Rs = 10, Da = 0.1, \zeta = 0.5, \eta = 0.5$  and  $\delta = 0.5$ .

The impact of  $Rs$  with three values of the Lewis number for the two categories when gravity fluctuation is  $h(z) = -(e^z - 1)$  and  $h(z) = \log(1 + z)$  is displayed in Figure 10. It is remarkable that with the rise of  $Rs$ , the critical Rayleigh number increases in the stationary mode. It illustrates the stabilizing effect of the gravitational fields of both types on stationary convection. In addition, we see that the Lewis number destabilizes the system.

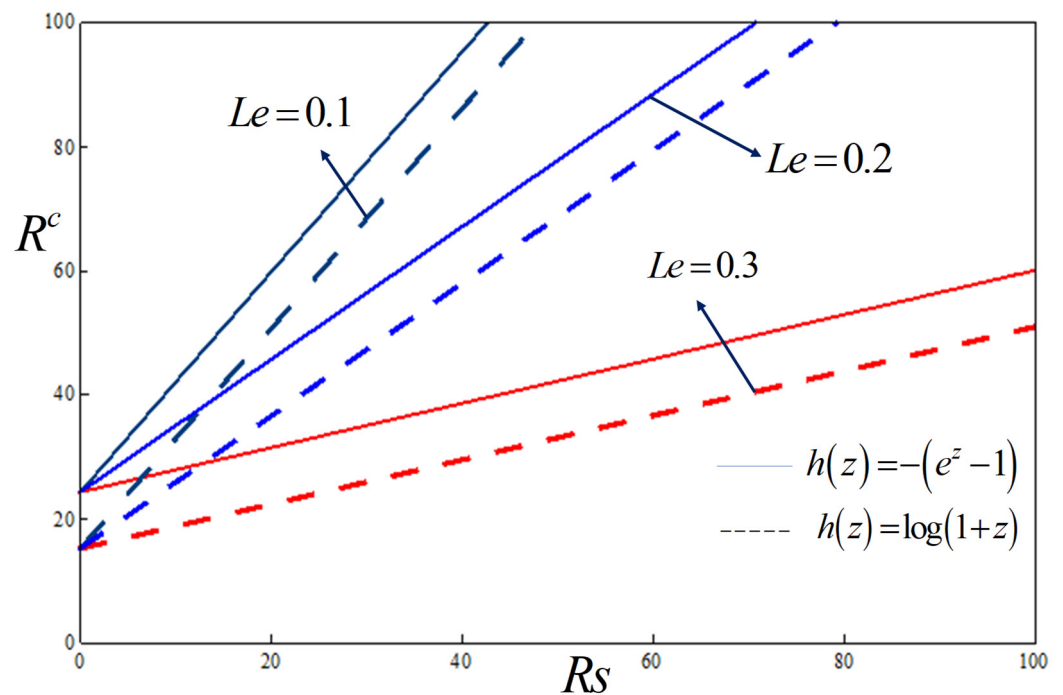


**Figure 10.** Plot of  $R^c$  versus  $Rs$  for two types of variable gravity functions for various values of  $Le$  with  $Rs = 10, Da = 0.1, \zeta = 0.5, \eta = 0.5$  and  $\delta = 0.5$ .

Figures 11 and 12 illustrate the effect of the Darcy number and  $Rs$  on critical Rayleigh numbers  $R^c$  for all six categories of the gravity field. Clearly, we notice from the figures that with an increase in  $Rs$ , the  $R^c$  increases for the stationary mode. Additionally, we

noted that the Darcy number has a stabilizing impact on the system. Furthermore, in case (iii), the gravitational field is more stable when compared to the remaining types of gravity variations.

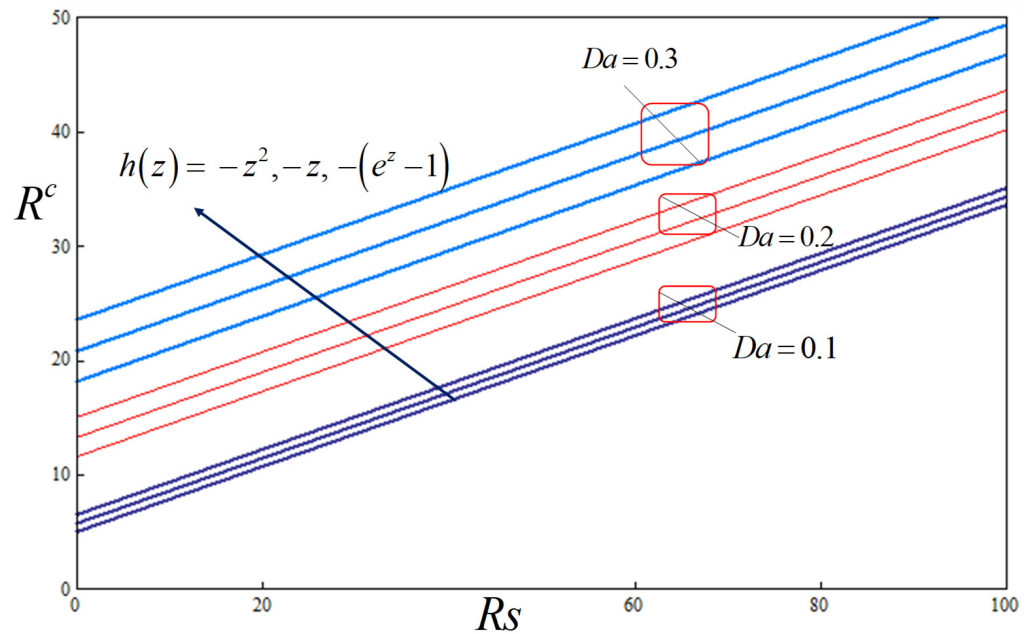


**Figure 11.** Plot of  $R^c$  versus  $Rs$  for different cases of negative variable gravity functions for various values of  $Da$  with  $Le = 0.5$ ,  $Rs = 10$ ,  $\zeta = 0.5$ ,  $\eta = 0.5$  and  $\delta = 0.5$ .

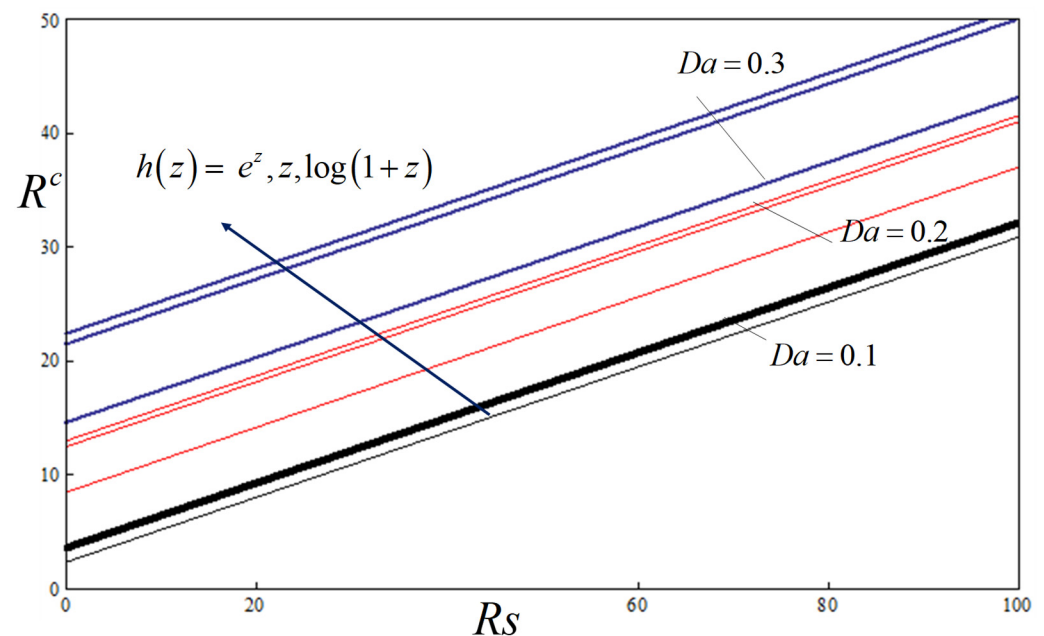


**Figure 12.** Plot of  $R^c$  versus  $Rs$  for three cases of negative gravity fluctuation for various values of  $Da$  with  $Le = 0.5$ ,  $Rs = 10$ ,  $Da = 0.1$ ,  $\zeta = 0.5$  and  $\delta = 0.5$ .

In Figures 13 and 14, the fluctuation of the stationary mode of  $R^c$  with  $Rs$  for various values of the mechanical anisotropy parameter  $\zeta$  for all six categories of the gravity field is demonstrated, with  $Rs = 10$ ,  $Da = 0.1$ ,  $\zeta = 0.5$ ,  $\eta = 0.5$  and  $\delta = 0.5$ . These graphs show that for all scenarios of a gravity field, the critical Rayleigh number drops as the mechanical anisotropy parameter  $\zeta$  increases. Additionally, we observe that the  $Rs$  has stabilizing effects on the system.

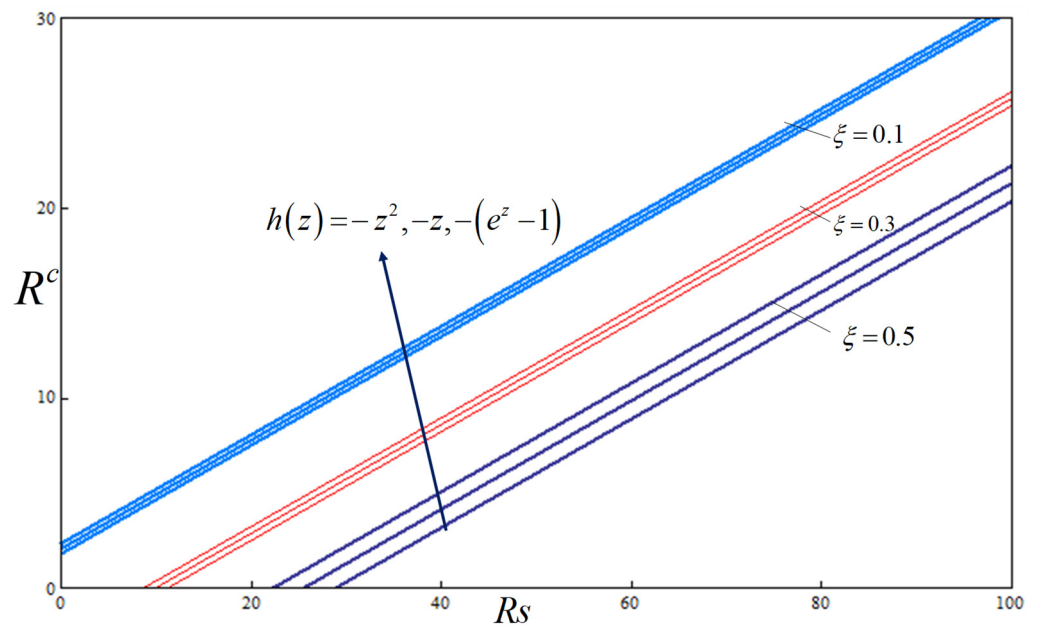


**Figure 13.** Plot of  $R^c$  versus  $Rs$  for three cases of negative gravity fluctuation for various values of  $\zeta$  with  $Le = 0.5, Rs = 10, Da = 0.1, \eta = 0.5$  and  $\delta = 0.5$ .

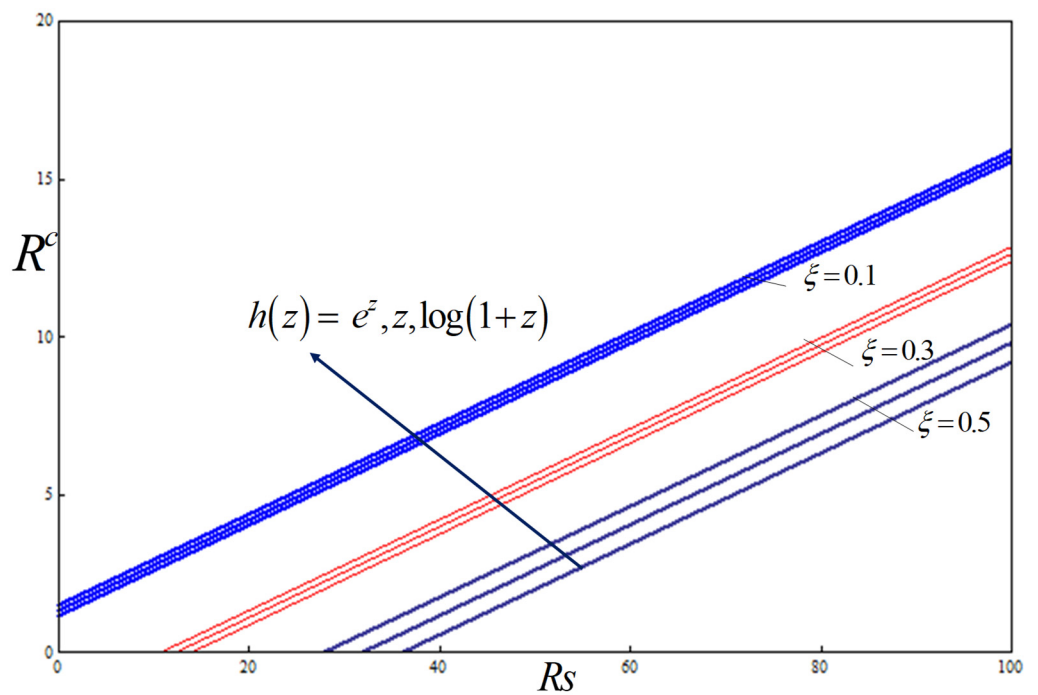


**Figure 14.** Plot of  $R^c$  versus  $Rs$  for three cases of positive gravity fluctuation for various values of  $\zeta$  with  $Le = 0.5, Rs = 10, Da = 0.1, \eta = 0.5$  and  $\delta = 0.5$ .

Figure 15 shows how the critical Rayleigh number for the stationary mode for decreasing types of gravity fields is affected by the thermal anisotropy parameter. As we can see, as  $\eta$  grows, the critical Rayleigh number also rises, and an increase in the value of  $\eta$  has the opposite effect, delaying the convective motion. Additionally, it was observed that in this case,  $\eta$  has the opposite effect to  $\zeta$ .

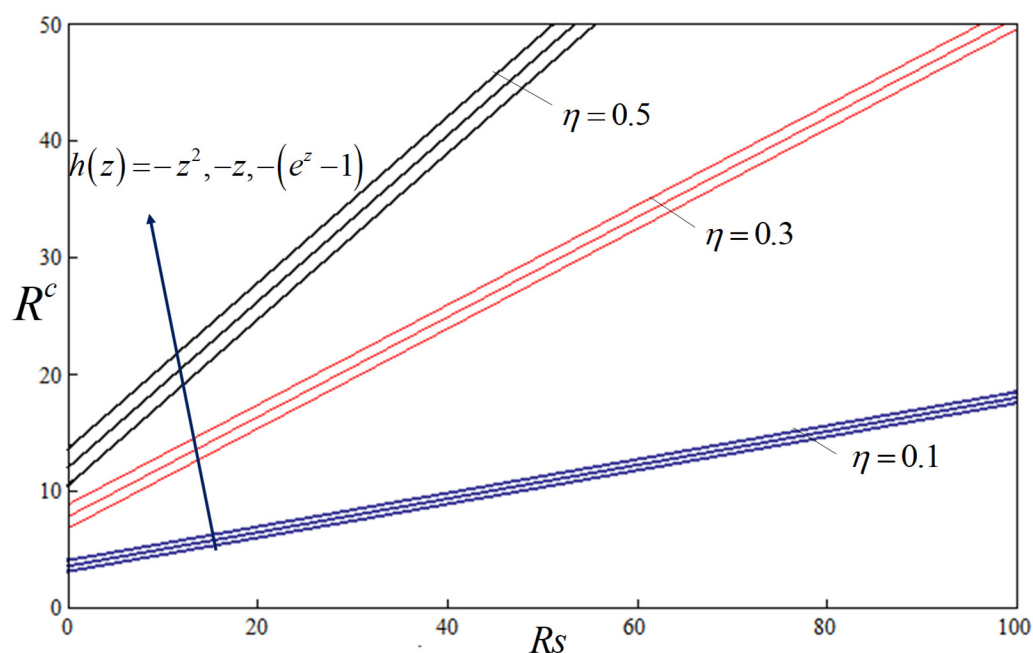


**Figure 15.** Plot of  $R^c$  versus  $Rs$  for different cases of positive variable gravity functions for various values of  $\eta$  with  $Le = 0.5$ ,  $Rs = 10$ ,  $\zeta = 0.5$ ,  $\eta = 0.5$  and  $\delta = 0.5$ .

## 6. Conclusions

The instability of a vertical constant throughflow in a horizontal anisotropic porous bed embedded in a changeable gravity field and filled by an electrically conducting double fluid mixture was performed. The single-term Galerkin weighted residuals method was employed to determine the critical Rayleigh numbers for the onset of steady and oscillatory instability. The six possible scenarios of the gravitational field were examined in the analysis: case (i)  $h(z) = -z$ , case (ii)  $h(z) = -z^2$ , case (iii)  $h(z) = -(e^z - 1)$ , case (iv)  $h(z) = e^z$ , case (v)  $h(z) = z$ , and case (vi)  $h(z) = \log(1 + z)$ . The convection of the system configuration is advanced in the presence of the Lewis number  $Le$ , mechanical anisotropy parameter  $\zeta$ , and gravity parameter for increasing types of gravity functions. Meanwhile, the effects of Darcy number  $Da$ , solutal Rayleigh number  $Rs$ , thermal anisotropy parameter  $\eta$ , throughflow parameter  $Q$ , and gravity parameter  $\delta$  for decreasing types of gravity functions stabilized the onset of thermosolutal convection. The configuration was noticed to be more unstable for case (ii) and more stable for case (vi) gravity variance. This research will undoubtedly be useful in the understanding of massive movements, such as the processing of materials, pollutant passage in saturated soils, the Earth's crust, atmosphere, and ocean, as well as fuel penetration, and crystal formation, for both injection and surjection, and can be crucial in controlling convective instability.

**Author Contributions:** Conceptualization, G.Y.H., M.N., N.H., and R.U.; methodology, G.Y.H. and M.N.; validation B.A., N.H., R.U., and A.M.E.; formal analysis, G.Y.H. and M.N.; investigation, R.U. and B.A.; writing—original draft preparation, G.Y.H., M.N., R.U., N.H., and A.M.E.; writing—review and editing, B.A.; visualization, All the authors; supervision, R.U. and M.N.; project administration, M.N. and R.U.; funding acquisition, B.A. All authors have read and agreed to the published version of the manuscript.

**Funding:** Princess Nourah bint Abdulrahman University Researchers Supporting Project number (PNURSP2023R216), Princess Nourah bint Abdulrahman University, Riyadh, Saudi Arabia.

**Institutional Review Board Statement:** Not applicable.

**Informed Consent Statement:** Not applicable.

**Data Availability Statement:** Not applicable.

**Acknowledgments:** Princess Nourah bint Abdulrahman University Researchers Supporting Project number (PNURSP2023R216), Princess Nourah bint Abdulrahman University, Riyadh, Saudi Arabia.

**Conflicts of Interest:** The authors declare no conflict of interest.

## Nomenclature

$a$	Horizontal wave number
$C$	concentration
$D = \frac{d}{dz}$	differential operator
$Da$	Darcy number
$g$	gravity
$G(z) = 1 + \delta h(z)$	variable gravity function
$h(z)$	Gravity fluctuations
$K$	Permeability
$Le = \frac{\kappa_s}{\kappa}$	Lewis number
$Pr = \frac{\nu}{\kappa}$	Prandtl number
$Q$	throughflow parameter
$R = \frac{\alpha g \Delta T d^3}{\nu \kappa}$	thermal Rayleigh number
$Rs = \frac{\rho_s g \Delta C d^3}{\nu \kappa_s}$	solutal Rayleigh number
$R^c$	Critical Rayleigh number
$S_r$	Soret parameter
$T$	temperature
$\vec{V}$	velocity vector
$W$	amplitude of perturbed vertical velocity
$w_0$	vertical throughflow velocity
$\zeta$	mechanical anisotropic parameter
$\eta$	thermal anisotropic parameter
$\rho$	density of the fluid
$\rho_0$	reference density of the fluid
$\kappa_s$	solutal diffusivity
$\mu$	Fluid viscosity
$\kappa$	diffusivity
$\sigma$	growth rate parameter
$\delta$	gravity parameter
$\Delta C$	characteristic Concentration difference
$\Delta T$	characteristic temperature difference

## References

- Castinel, G.; Combarous, M. Critère d'apparition de la convection naturelle dans une couche poreuse anisotrope. *Comptes Rendus Hebdomadaires des Séances de l'Académie des Sciences. Série B* **1974**, *278*, 701–704.
- Epherre, J.F. Critère d'apparition de la convection naturelle dans une couche poreuse anisotrope. *Rev. Gen. Therm.* **1975**, *168*, 949–950.
- Palm, E.; Tyvand, P.A. Thermal convection in a rotating porous layer. *Z. Angew. Math. Phys.* **1984**, *35*, 122–123. [[CrossRef](#)]
- Malashetty, M.S.; Mahantesh Swamy. The onset of convection in a binary fluid-saturated anisotropic porous layer. *Int. J. Therm. Sci.* **2010**, *49*, 867–878. [[CrossRef](#)]
- Govinder, S. Coriolise effect on the stability of centrifugally driven convection in a rotating anisotropic porous layer subject to gravity. *Transp. Porous Media* **2007**, *69*, 55–66. [[CrossRef](#)]
- Shivakumara, I.S.; Mamatha, A.L.; Ravisha, M. Local thermal non-equilibrium effects on thermal convection in a rotating anisotropic porous layer. *Appl. Math. Comput.* **2015**, *259*, 838. [[CrossRef](#)]
- Degan, G.; Vasseur, P.; Bilgen, E. Convective heat transfer in a vertical anisotropic porous layer. *Int. J. Heat Mass Transf.* **1995**, *38*, 1975–1987. [[CrossRef](#)]
- Payne, L.E.; Rodrigues, J.F.; Straughan, B. Effect of anisotropic permeability on Darcy's law. *Math. Methods Appl. Sci.* **2001**, *24*, 427–438. [[CrossRef](#)]
- Rees, D.A.S.; Postelnicu, A. The onset of convection in an inclined anisotropic porous layer. *Int. J. Heat Mass Transf.* **2001**, *44*, 4127–4138. [[CrossRef](#)]
- Yadav, D.; Kim, M.C. Theoretical and numerical analyses on the onset and growth of convective instabilities in a horizontal anisotropic porous medium. *J. Porous Media* **2014**, *17*, 1061–1074. [[CrossRef](#)]

11. Mahajan, A.; Nandal, R. Anisotropic porous penetrative convection for a local thermal non-equilibrium model with Brinkman effects. *Int. J. Heat Mass Transf.* **2017**, *115*, 235–250. [[CrossRef](#)]
12. Alex, S.M.; Patil, R. Effect of variable gravity field on thermal instability in a porous medium with inclined temperature gradient and vertical throughflow. *J. Porous Media* **2002**, *5*, 137–147. [[CrossRef](#)]
13. Rionero, S.; Straughan, B. Convection in a porous medium with internal heat source and variable gravity effects. *Int. J. Eng. Sci.* **1990**, *28*, 497–503. [[CrossRef](#)]
14. Gangadharaiah, Y.H.; Suma, S.P.; Ananda, K. Variable gravity field and throughflow effects on penetrative convection in a porous layer. *Int. J. Comput. Technol.* **2013**, *5*, 172–191.
15. Suma, S.P.; Gangadharaiah, Y.H.; Indira, R. Effect of throughflow and variable gravity field on thermal convection in a porous layer. *Int. J. Eng. Sci. Tech.* **2011**, *3*, 7657–7668.
16. Gangadharaiah, Y.H.; Nagarathnamma, H.; Hanumagowda, B.N. Combined impact of vertical throughflow and gravity variance on Darcy-Brinkman convection in a porous matrix. *Int. J. Thermofluid Sci. Technol.* **2021**, *8*, 080303.
17. Yadav, D. Numerical investigation of the combined impact of the variable gravity field and throughflow on the onset of convective motion in a porous medium layer. *Int. Commun. Heat Mass Transf.* **2019**, *108*, 104274. [[CrossRef](#)]
18. Gangadharaiah, Y.H.; Ananda, K.; Aruna, A.S. Effects of throughflow on thermosolutal penetrative convection in a fluid layer with a variable gravity field. *Heat Transf.* **2022**, *51*, 7584–7596.
19. Mahabaleshwar, U.S.; Basavaraja, D.; Wang, S.; Lorenzini, G.; Lorenzini, E. Convection in a porous medium with variable internal heat source and variable gravity. *Int. J. Heat Mass Transf.* **2017**, *111*, 651–656. [[CrossRef](#)]
20. Mahajan, A.; Tripathi, V.K. Effects of spatially varying gravity, temperature and concentration fields on the stability of a chemically reacting fluid layer. *J. Eng. Math.* **2020**, *125*, 23–45. [[CrossRef](#)]
21. Yadav, D.; Bhargava, R.; Agrawal, G.S. Boundary and internal heat source effects on the onset of Darcy-Brinkman convection in a porous layer saturated by nanofluid. *Int. J. Therm. Sci.* **2012**, *60*, 244–254. [[CrossRef](#)]
22. Yadav, D.; Lee, J.; Cho, H.H. Brinkman convection induced by purely internal heating in a rotating porous medium layer saturated by a nanofluid. *Powder Technol.* **2015**, *286*, 592–601. [[CrossRef](#)]
23. Yadav, D. The onset of Darcy-Brinkman convection in a porous medium layer with vertical throughflow and variable gravity field effects. *Heat Transf.* **2020**, *49*, 3161–3173. [[CrossRef](#)]
24. Bhadauria, B.S. Double-diffusive convection in a saturated anisotropic porous layer with internal heat source. *Transp. Porous Med.* **2012**, *92*, 299–320. [[CrossRef](#)]
25. Siddheshwar, P.G.; Bhadauria, B.S.; Srivastava, A. An analytical study of nonlinear double-diffusive convection in a porous medium under temperature/gravity modulation. *Transp. Porous Med.* **2012**, *91*, 585–604. [[CrossRef](#)]
26. Deepika, N.; Anjana Matta; Lakshmi Narayana, P.A. Effect of throughflow on double diffusive convection in a porous medium with concentration based internal heat source. *J. Porous Media* **2016**, *19*, 303–312. [[CrossRef](#)]
27. Gaikwad, S.N.; Rangdal, P.B. Effect of gravity and throughflow on double diffusive convection in a couple stress fluid saturated porous media. *J. Adv. Res. Fluid Mech. Therm. Sci.* **2023**, *101*, 121–136. [[CrossRef](#)]
28. Malashetty, M.S.; Biradar, B.S. The onset of double-diffusive reaction-convection in an anisotropic porous layer. *Phys. Fluids* **2011**, *23*, 064102. [[CrossRef](#)]

**Disclaimer/Publisher's Note:** The statements, opinions and data contained in all publications are solely those of the individual author(s) and contributor(s) and not of MDPI and/or the editor(s). MDPI and/or the editor(s) disclaim responsibility for any injury to people or property resulting from any ideas, methods, instructions or products referred to in the content.